

# Characterization of the Surface Alteration Layer in 19<sup>th</sup>-Century Potassium Silicate Glass

## ABSTRACT

*Models of alkali glass deterioration are generally based on the concept that glass formulated with network modifiers such as potassium and sodium ions, and lacking in sufficient stabilizers, undergoes alkali leaching upon exposure to moisture. This process entails formation of a hydrated “gel” layer at the glass surface, the exact nature of which is difficult to characterize in historical glass objects. The chemical and physical properties of the altered surface layer are critical to treatment decisions. The purpose of this paper is to apply and compare several tools for the characterization of the alteration layer in individual potassium silicate glass objects from the 19<sup>th</sup> century in order to improve our current ability to assess and understand their condition.*

## KEYWORDS

Potash glass · Deterioration · pH ·  
Raman spectroscopy · X-ray diffraction ·  
BSE-SEM/EDS · Fiber optics reflectance spectroscopy ·  
Optical coherence tomography

## INTRODUCTION

Descriptions of alkali silicate glass deterioration proliferate in the conservation and scientific literature due to the common occurrence of 19<sup>th</sup>-century glass formulations with alkali-based network modifiers and without sufficient stabilizers, such as calcium oxide (CaO) or lead oxide (PbO). In particular, a brief review of the literature illustrates the widely-held postulate that high-potassium (K) glass (potash glass) deterioration involves the hydration of the glass matrix, subsequent hydrogen ion/potassium ion (H<sup>+</sup>/K<sup>+</sup>) interdiffusion, leaching of K, and generation of potassium hydroxide (KOH) that leads to hydrolysis of the silicate network (Brill 1972; Brill 1975; Hench and Clark 1978; Clark and Zaitos 1992; White 1992; Bunker 1994; Kunicki-Goldfinger 2002; Farges et al. 2006; Kunicki-Goldfinger 2008; Fletcher et al. 2008; Rodrigues et al. 2018).

The resulting hydrated glass surface is often referred to as a gel layer, although its description varies and is usually not distinguished for K as opposed to sodium (Na) silicate glass (Hench and Clark 1978; Ryan 1995; Newton and Davison 2003; Fearn 2006). Prolonged exposure to

## AUTHORS

**Lynn Brostoff\***  
Senior Scientist  
Library of Congress  
lbrostoff@loc.gov

**Carol Lynn Ward-Bamford**  
Curator of Musical Instruments  
Library of Congress  
cwar@loc.gov

**Stephanie Zaleski**  
Postdoctoral Fellow  
Biomedical Engineering Department  
George Washington University  
stephanie.zaleski@northwestern.edu

**Elizabeth Montagnino**  
Graduate Student  
Vitreous State Laboratory,  
Catholic University of America  
36montagnino@cua.edu

**Andrew Buechele**  
Vitreous State Laboratory  
Catholic University of America  
andrewb@vsl.cua.edu

**Isabelle Muller**  
Vitreous State Laboratory  
Catholic University of America  
isabellem@vsl.cua.edu

**Tara Diba**  
Graduate Student  
Biomedical Engineering Department  
George Washington University  
taradiba@gwmail.gwu.edu

**Jason Zara**  
Associate Professor  
Biomedical Engineering Department  
George Washington University  
jasonzara@gmail.com

**Murray Loew**  
Professor  
Biomedical Engineering Department  
George Washington University  
loew@gwu.edu

**Fenella France**  
Chief of Preservation Research  
and Testing Division  
Library of Congress  
frfr@loc.gov

\*Corresponding Author

fluctuations in humidity are commonly held to be responsible for visible symptoms of deterioration, including cracking, flaking, and spalling of the gel layer (Kunicki-Goldfinger 2008). As a guide for conservators, alkali silicate glass deterioration is also defined in terms of five progressive stages of “crizzling.” This system of visual observation defines the initial stage as a “cloudy or hazy appearance due to alkali salts or liquid droplets on the surface,” subsequent “incipient crizzling” as microscopic cracking resembling “silvery lines,” and three advanced stages of readily observable cracking (Koob 2006; Koob 2012).

The current conservation approach to caring for deteriorating historical glass often involves cleaning in order to remove the perceived caustic alteration layer as a stabilization intervention (Koob 2004; Koob 2006; Koob et al. 2018; Newton and Davison 2003; Fletcher et al. 2008). Understanding the chemical and physical properties of the surface region on individual objects is thus critical to making informed treatment decisions. This study applies and compares tools for the characterization of the alteration layer using glass flutes, musical instruments produced by Claude Laurent of Paris in the first half of the 19<sup>th</sup> century, as subjects.

The Library of Congress (LC) holds 21 Laurent glass flutes as part of its Dayton C. Miller Collection (DCM). As previously reported (Laurent Glass Flutes; Buechele et al. 2015; Ward-Bamford et al. 2019), technical analysis of these and other Laurent flutes worldwide has revealed that most are formulated with approximately 12–18 atomic weight percent (at.wt.%) K, 2–3 at.wt.% Ca, and remaining elements other than silicon (Si) less than about 0.2 at.wt.%. This potash glass was clearly made as a type of imitation “crystal.” The latter designation is associated with Laurent’s production due to his patent award for *flûtes en cristal*, i.e., for leaded glass flutes, in 1806 (Laurent Patent 1806). To date, however, only two out of 45 Laurent flutes examined have proved to be leaded glass, with an additional five flutes and piccolos having one or more leaded glass joints. With this knowledge, it is unsurprising that the bulk of his output now shows signs of deterioration.

This paper focuses on analytical results obtained for two representative flutes, DCM 717 and DCM 1681, plus model glass of approximately the same

composition as DCM 717 with 16.8 at.wt.% K, 0.7 at.wt.% Na, and 2.5 at.wt.% Ca. Methods utilized here include light microscopy, surface pH, Raman spectroscopy (Raman), quantitative elemental analyses by X-ray fluorescence spectroscopy (XRF), X-ray diffraction (XRD), backscattered electron scanning electron microscopy and energy dispersive X-ray spectroscopy (BSE-SEM/EDS), fiber optics reflectance spectroscopy (FORS), and optical coherence tomography (OCT).

## METHODS

A group of replica glass samples was modeled on the composition of DCM 717 and designated S-717 (2015 experiment) or Flute 1 (F-1) (2017 repeat experiment). The manufacture was as follows: the raw materials were twice-melted and quenched; to cast as thin disks, glass fragments were collected from the small platinum gold alloy mold and placed in shallow platinum crucibles in a pre-heated furnace at 1250 °C for one hour; and the crucibles were transferred to a different furnace initially set to 625 °C and cooled at a rate of 7 °C per hour, annealing the glass to relieve stresses and prevent fractures. Some samples were difficult to free from the mold, thus creating small stress fractures and additional roughness on the crucible contact sides. Resulting glass “coins” measured approximately 3–4 mm thick, with one crucible side and one air-annealed surface. Artificial aging of the model glass was conducted in a Parameter Generation and Control Inc. controlled temperature and humidity environmental chamber at 90 °C and 90 percent relative humidity (RH). Quantitative elemental analysis of replica glass samples was conducted using a PANalytical Axios<sup>mAX</sup>-Advanced X-ray fluorescence (XRF) spectrometer, calibrated using standard reference materials.

One microsample from DCM 717 and samples from the model glasses were epoxy-mounted, cross-sectioned, and analyzed by BSE-SEM/EDS using a JEOL JSM-5910 SEM outfitted with an Oxford EDS detector and operated at 20 kV accelerating voltage, 0.45 nA probe current, 60 seconds X-ray collection live time, 10 mm working distance, and 20 µm objective aperture. INCA software was used for quantitative microanalysis, the results of which are expressed here in at.wt.% in order not to make assumptions about oxidation states.



**Figure 1.** Claude Laurent, Flute in C, ca. 1815 CE, glass, silver, mother-of-pearl, L 61.7 cm × W 66.9 cm. Library of Congress, DCM 717 · Courtesy of Library of Congress · Photomicrographs of DCM 717 (below, left to right): exterior of head joint, cracking and spalling; interior of head joint, severe network cracking; exterior of foot joint, fine network microcracking; interior of extra foot joint, fine, parallel microcracking; interior of extra foot joint, rough polished surface with no visible deterioration

Surface pH measurements were conducted on separate areas of the samples using colorpHast pH indicator strips, where the pH strip was wetted with deionized water and held to the surface of the glass sample for two minutes. A second method involved using a pH meter measurement on a droplet of deionized water applied to the glass surface. All pH measurements were taken at random areas on the sample surfaces. The pH strip method was previously used to collect readings for the DCM flutes.

Raman spectra of particulates from DCM flutes and model samples were obtained using a Renishaw inVia Raman system outfitted with a Leica DM2500 microscope, a 514 nm argon ion laser and 2400 lines/mm grating or a 785 nm diode laser and 1200 lines/mm grating, Rayleigh notch filters, and a charge-coupled device detector. Spectra were calibrated to the 520.5  $\text{cm}^{-1}$  line of silicon.

XRD of surface samples was performed on a Rigaku D/Max Rapid outfitted with an image plate area detector and run with copper (Cu) K $\alpha$  ( $\lambda = 1.54 \text{ \AA}$ ) radiation at 1.20 kW using a 0.3 mm collimated beam; goniometer parameters were  $\chi$  fixed at 45°,  $\omega$  fixed at 0°, and  $\phi$  360° rotation. Patterns were integrated with Rigaku 2DP software and qualitatively matched using PDXL software and the 2016 International Center for Diffraction Data database.

FORS spectra were taken using a FieldSpec4 from PANalytical using an approximately 3 mm collection fiber and handheld light source at a roughly 45° angle to each other, approximately 1-2 cm above the object. Spectra were acquired in the range of 350-2500 nm, spanning the visible and near-short infrared (NIR-SWIR) regions. Spectra were normalized to a Spectralon white 100 percent reflectance standard. Raw FORS data were converted to second-derivative spectra for peak intensity comparison between spectra at maxima.

OCT was conducted with a ThorLabs, Inc. spectral domain, Fourier-domain Ganymede II system utilizing a center wavelength of 930 nm. The instrument has an axial resolution in air of 6.0  $\mu\text{m}$ , lateral resolution of 8.0  $\mu\text{m}$ , and A-scan rate of 5.5-36 kHz. Each 2D OCT image was generated from an average of ten A-scans across the surface. Physical scaling was corrected for data reported here using a measured refractive index of 1.45.

## RESULTS

### Visual assessment of the surface

Various levels of deterioration are found among the DCM Laurent potash glass flutes. This can be related both to the objects' compositions and specific history of environmental exposure and use, including direct contact with the player's skin, breath, and spittle, such as at upper joints.

MODEL SAMPLE	DAYS AGED AT 90 °C, 90 %RH	APPROX. STORAGE TIME	SAMPLE SIDE, TREATMENT	pH METER READING	pH STRIP READING*	VISUAL APPEARANCE OF DETERIORATION
F-1	0	None	Air	9.3	--	--
F-1	0	None	Crucible	9.2-9.7	--	--
F-1	1	None	Air	10.3	9	--
F-1	1	None	Crucible	10.8-11.1	10.5	Visible cracking
F-1	2	None	Air	10.1	9.5-10.0	--
F-1	2	None	Crucible	11.7	11.5	Severe cracking and surface opacity
F-1	3	None	Air	10.7	10.0-10.5	Edge cracking
F-1	3	None	Crucible	11.6	11.5-12.0	Severe cracking and surface opacity
S-717	0	2 years	Air	9.2	8.0-8.5	--
S-717	0	2 years	Air, ethanol rinse	9.1	8.5	--
S-717	0	2 years	Crucible	9.3	--	--
S-717	0	2 years	Crucible, ethanol rinse	6.9-8.9	--	--
S-717	9	2 years	Air	10.3	9.5	Some cracking
S-717	9	2 years	Air, ethanol rinse	10.2	9.0-9.5	Some cracking
S-717	9	2 years	Crucible	9.8	9.5-10.0	Severe cracking and surface opacity
S-717	9	2 years	Crucible, ethanol rinse	10.2	9.5-10.0	Severe cracking and surface opacity

**Table 1.** Surface pH of model potash glass aged at 90 °C and 90 percent RH

\*pH strip data for some samples not available due to small size of samples

For example, DCM 717 has severe deterioration, including dense network cracking and spalling on both exterior and interior surfaces of the head joint (HJ) and upper body joints (UBJ) (Figure 1). These visible manifestations of deterioration are responsible for varying degrees of opacity to the naked eye. Low magnification, up to 70x, is necessary to discern fine microcracking on the lower body joint (LBJ), and, even with magnification, it is difficult to discern the isolated fine, parallel cracks on the foot joint (FJ) and damaged extra foot joint (xFJ) (Figure 1). On all

joints, surface particulates are sparse or non-existent, and no droplets are observed. These observations are typical of other DCM flutes.

The artificial aging of S-717 and F-1 model glass, carried out at 90 °C and 90 percent RH roughly two years apart, produces visual deterioration quite similar to the flutes (Buechele et al. 2015; Ward Bamford et al. 2019; Brostoff et al. in press; Zaleski et al. 2019). Cracking patterns are reproduced fairly faithfully, progressing during aging from linear, scattered cracking to dense



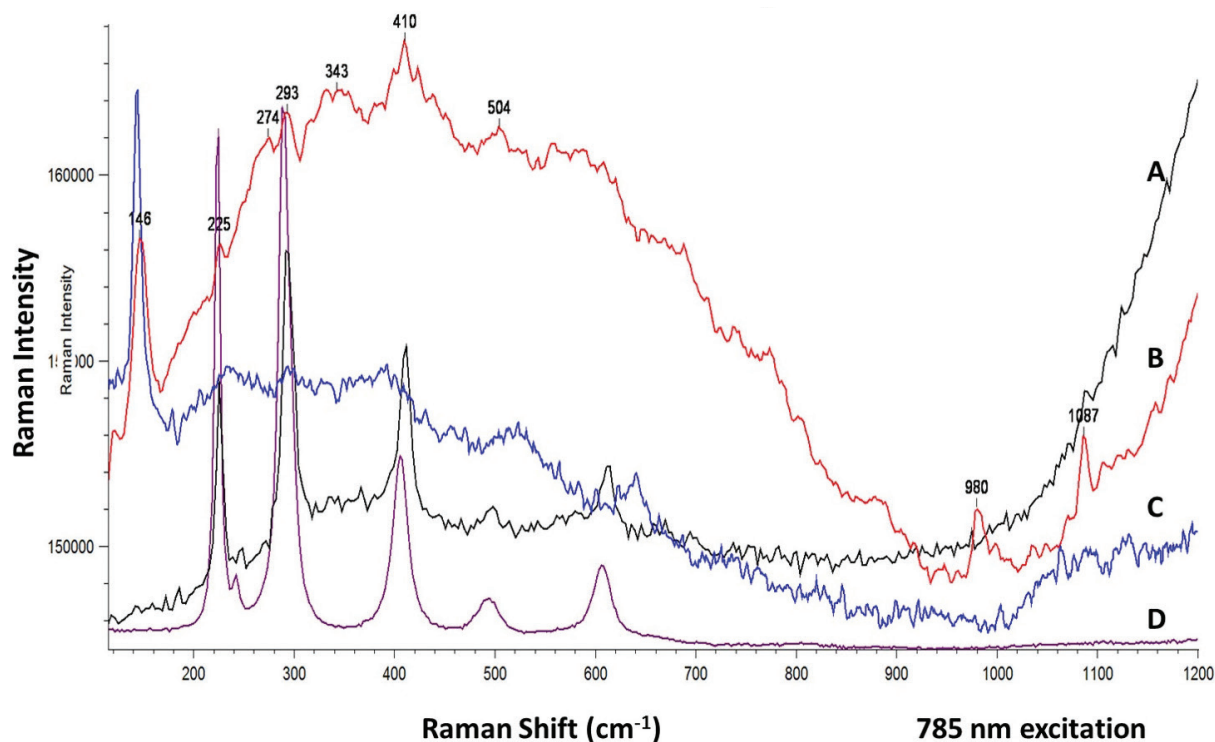


Figure 2. Raman spectra of particulates sampled from DCM 717 (A,B), DCM 1235 (C), and DCM 450 (D)

network cracking, which renders the samples opaque-looking. No obvious precipitates are formed, and some cracking is observed to have occurred before removal from the aging chamber.

### Surface pH

Average pH readings previously taken from the entire collection of DCM flute glass surfaces using pH strips were variable, ranging from 6.5 to 9.5; these readings often do not correlate with visible condition. pH readings of model glass surfaces by two methods (described above) show a more consistent upward trend with artificial aging, and support visual assessment that deterioration is more accelerated on the crucible sides of the samples, possibly due to residual stresses (Table 1). It is unclear why the pH on these samples registers as alkaline on the unaged surfaces, even before extended storage. Data does suggest that pH tends to level off during extended aging and storage, supported by pH measurements on sample S-717. pH sampling method development is ongoing.

### Analysis of surface species

Select Raman analysis of visible particulates sampled from different flutes is shown in Figure 2.

In these spectra, intense peaks near 144-146  $\text{cm}^{-1}$  indicate anatase, probably with some rutile, while intense peaks near 225, 293, 410, 500, and 612  $\text{cm}^{-1}$  indicate hematite; peaks near 983 and 1087  $\text{cm}^{-1}$  indicate an unidentified sulfate and calcite, respectively. As exemplified here, Raman analysis suggests that visible particulates on the flutes are mostly polishing debris, as well as extensive dirt, rather than alkali salts. This result illustrates that benign surface particulates can be confused with deterioration products, specified in the “stages of crizzling” as indicating “stage 1” deterioration (Koob 2006). Select XRD analysis of clear surface scrapings mounted on a wooden stick (and thus air-dried), on the other hand, reveals the presence of potassium chloride (KCl) and potassium sulfate ( $\text{K}_2\text{SO}_4$ ) in a few cases, including on the severely degraded DCM 717 (Figure 3). This supports the contention that deteriorated glass surfaces contain reactive potassium species, although they do not necessarily precipitate as *visible* crystals. In addition, Raman analysis of material observed within the cracks of some model samples identified potassium bicarbonate particles (not shown). This result provides a partial explanation for cracking, in addition to volume increase from water ingress and wet/dry cycling (Palomar et al. 2017). While

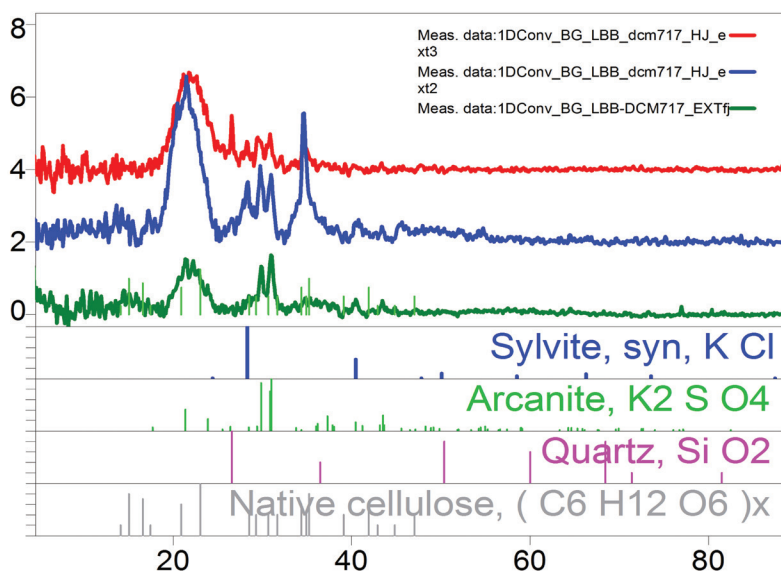


**Figure 3.** XRD patterns from surface material sampled from the exterior surface of DCM 717 head and extra foot joints with phase identifications; peaks near  $2\theta=20$  and  $2\theta=34.7$  are artifacts of the wood sampling stick

lack of visible surface precipitates in general on the flutes may partly be ascribed to periodic cleaning during use, it should be noted that according to records, the collection has not undergone cleaning, with one possible exception, since they were donated in 1941.

### BSE-SEM/EDS

BSE-SEM analysis of cross-sections allows direct visualization of the gel layer, although this invasive method is rarely undertaken on historical objects. Analysis of a cross-section from the damaged DCM 717 xFJ reveals approximately 30  $\mu\text{m}$  thick alteration layers on both the external and internal surfaces (Figure 4) (Buechele et al. 2015). The image shows a remarkably homogeneous and sharply-defined alkali-depleted subsurface; EDS analysis further shows that K decreases from about 17.4 at.wt.% in the bulk glass to about 6.5 at.wt.% in the surface region.

BSE-SEM/EDS analysis of cross-sections from model glass samples artificially aged from zero to seven days shows that the observed degree of surface cracking increases with the thickness of the depletion layer (Figure 5a-b), varying linearly with aging time, as previously reported (Buechele et al. 2015). The morphology of the depletion layer has the homogeneous, uniform appearance seen

on DCM 717 (Figure 4) (Ward-Bamford et al. 2018). The image also shows that the F-1 seven-day aged sample has significant cracking below the alkali-depleted layer (Figure 5b).

### FORS (SW-NIR spectroscopy)

Non-invasive FORS is quite sensitive to molecular bond vibrations from water ( $\text{H}_2\text{O}$ ) and hydroxyl ion ( $\text{OH}^-$ ) species in the NIR region. Results for model glass samples and the DCM Laurent flutes are compelling in showing a direct and sensitive measurement of hydration in the glass through absorption features near 1410 and 1910 nm, where the peak near 1410 nm is assigned to a combination vibrational band of  $\text{OH}^-$  and  $\text{H}_2\text{O}$ , and the peak near 1910 nm is characteristic of isolated, bound  $\text{H}_2\text{O}$  in the silicate matrix (Clark 1999; Rice et al. 2013). The absorption near 1910 nm, a more intense feature, progressively increases with time of aging on the F-1 model samples (Figure 5c), and can be detected in model glass samples with an alteration layer as thin as 0.66  $\mu\text{m}$ , as measured by BSE-SEM. Application of FORS for assessment of glass condition in the DCM Laurent flutes also correlates to the observed relative deterioration, and, most importantly, allows assessment of potash flutes without visible deterioration. This work is the subject of ongoing investigation and separate publications (Zaleski et al. 2019).

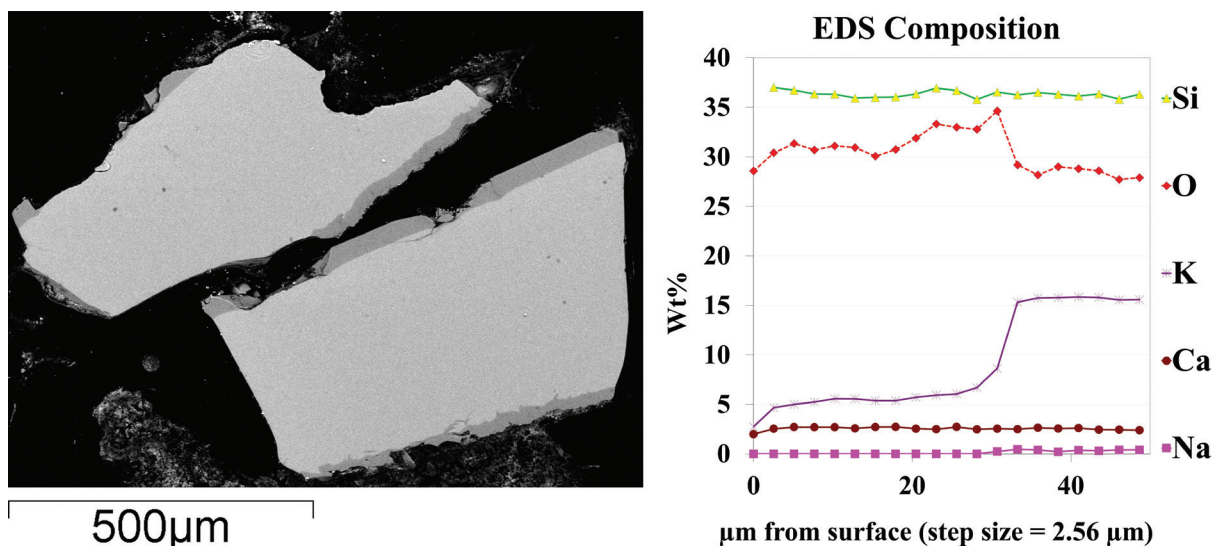


Figure 4. BSE-SEM image (left) of cross-sections sampled from DCM 717 Laurent flute, and plot (right) of EDS compositional results for depletion layer and bulk glass areas of cross-section as a function of distance from the outermost surface into the bulk glass. Previously reproduced in Buechele et al.

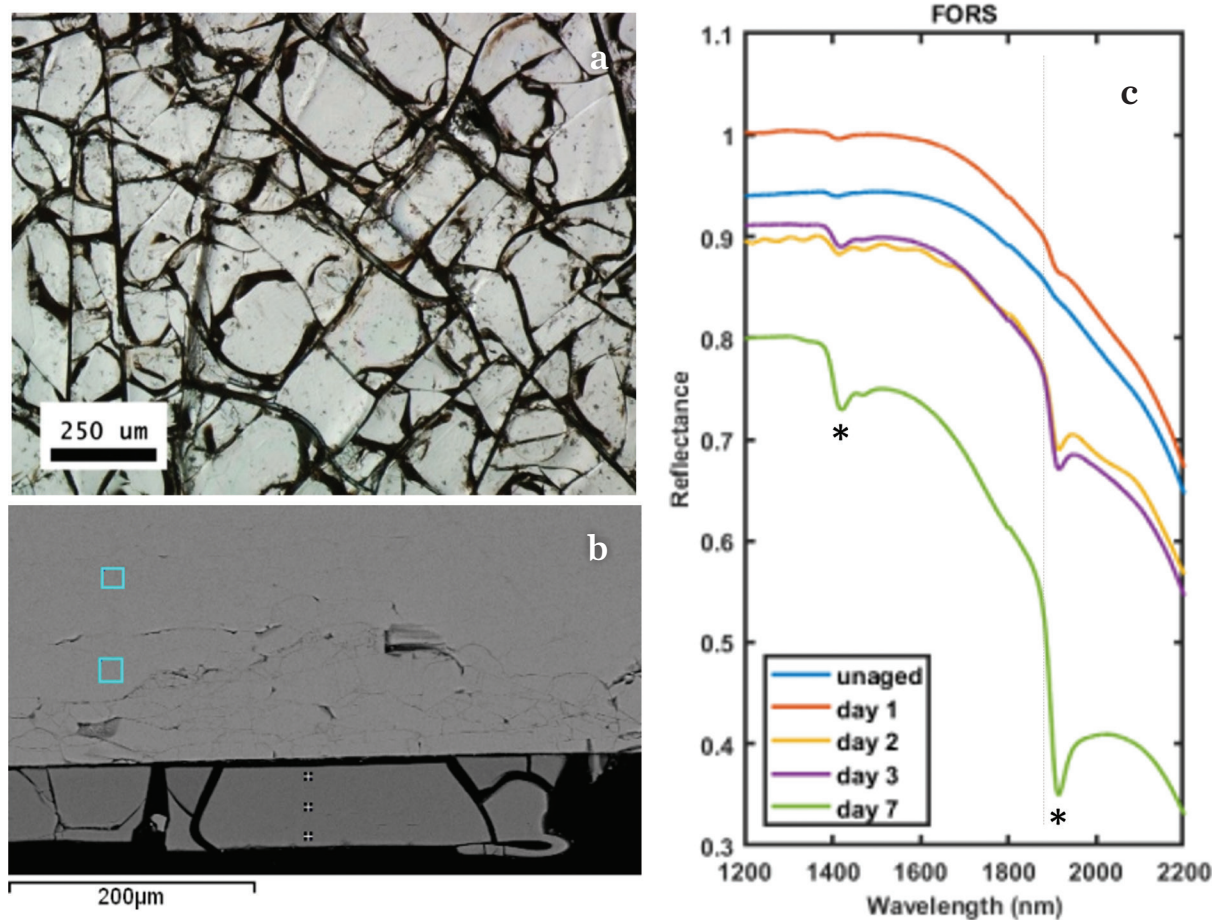
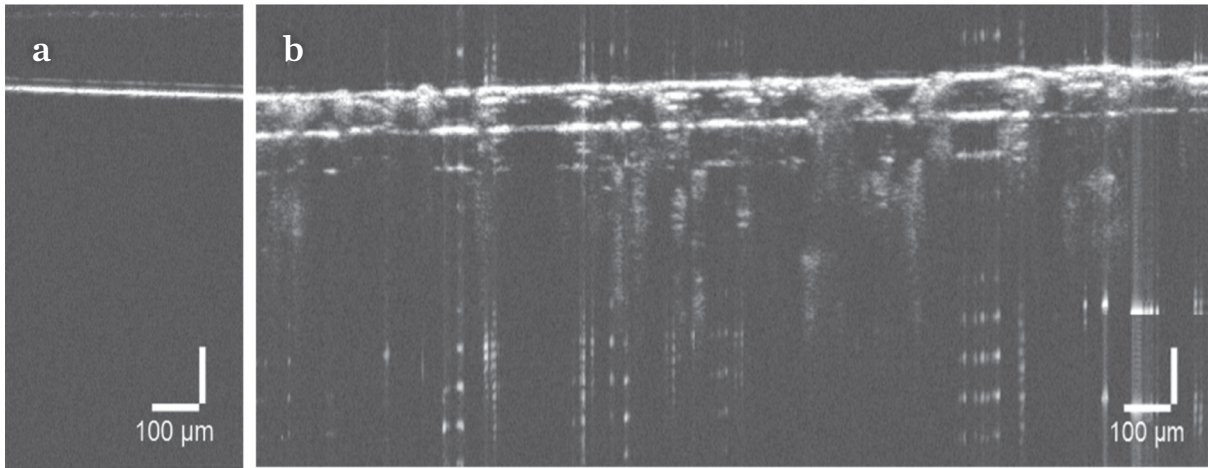
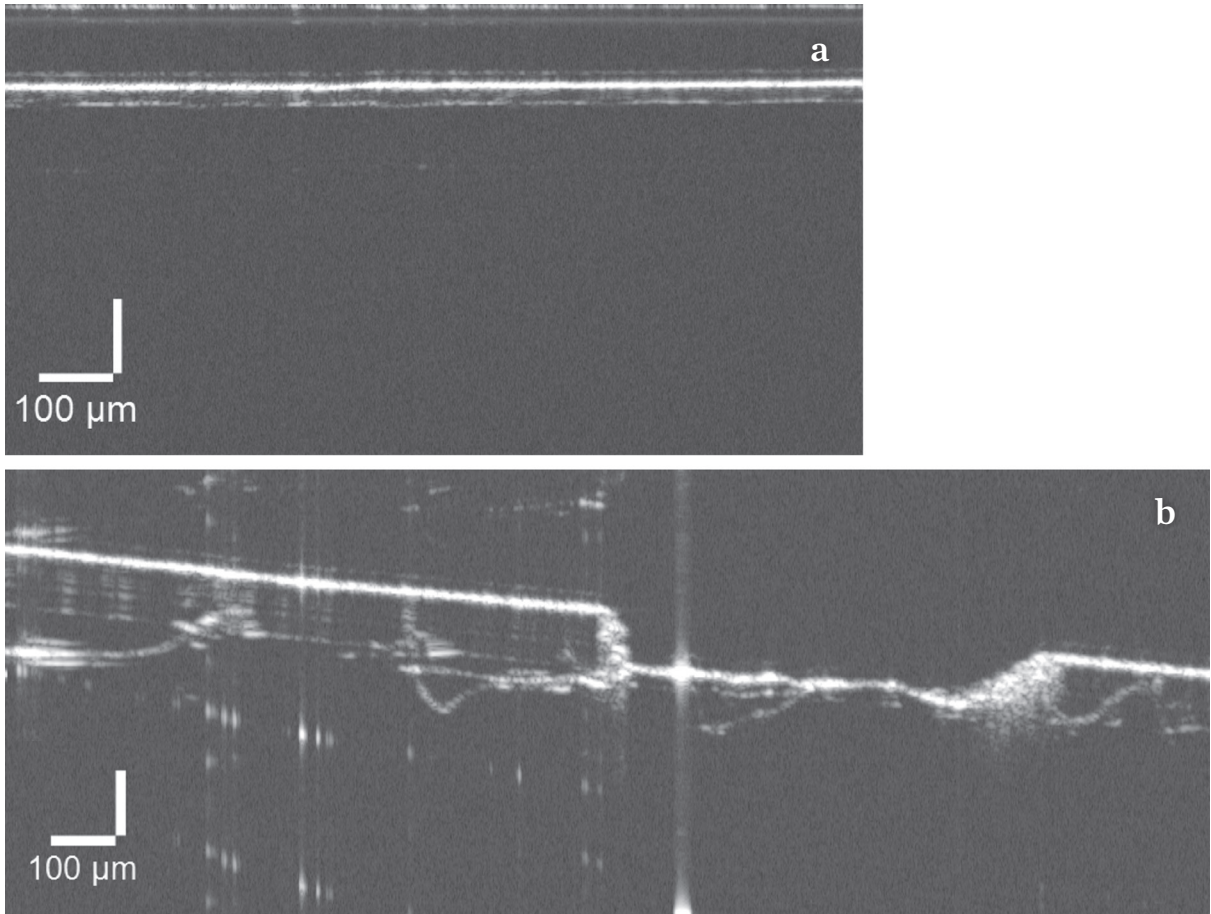


Figure 5. Comparative results for F-1 model potash glass sample, crucible side, aged at 90 °C and 90 percent RH: a) light micrograph after seven days aging, b) BSE-SEM image of cross-section after seven days aging with squares marking areas of EDS analysis, and c) FORS reflectance spectra from zero to seven days aging, with features near 1410 and 1910 nm marked with asterisks





**Figure 6.** OCT images of F-1 model potash glass sample, crucible side, a) without aging and b) with artificial aging at 90 °C and 90 percent RH for seven days



**Figure 7.** OCT images of a) DCM 717 flute extra foot joint and b) DCM 1681 flute head joint



## OCT

OCT is an optical imaging technique that uses partially coherent NIR light to create high-resolution cross-sectional profiles of sub-surface microscopic structures approximately 2-3 mm deep. The image features arise primarily from differences in refractive indices at boundaries such as air/glass interfaces, where refractive index changes from 1.00 to approximately 1.50, respectively. This causes the scattering of light; signal response may also arise from backscattering on rough-textured features. Applied to glass (Kunicki-Goldfinger et al. 2009), the technique allows non-invasive 2D and 3D imaging of the glass surface and glass/air interfaces at cracks beneath the surface. Reflections from the bulk glass/hydrated glass interface can potentially be detected as well. Explorations of the potential value and limitations of this technique as applied to historical glass, including identification of image artifacts, are ongoing and the subject of another publication (Brostoff et al. in press).

OCT images of the crucible sides of unaged and aged model glass F-1 is shown in Figure 6. The 2D profile of the zero-day aged sample (Figure 6a) simply shows a bright line that demarcates the air/glass interface (with a lighter artifact line above), while that of the crucible side of the seven-day aged sample (Figure 6b) shows a clear subsurface layer approximately  $70 \pm 7 \mu\text{m}$  thick, with a fairly regular sequence of angled cracks within the layer. Reflections from deep cracks below the alteration layer are also indicated. Within the margin of error of either technique, the alteration layer thickness corresponds well to the depletion layer thickness measured on the same sample by BSE-SEM, approximately  $65 \pm 9 \mu\text{m}$  (Figure 5).

Comparison between OCT-visualized alteration in two spots and SEM-determined depletion layers in the DCM 717 xFJ shows excellent agreement, with a relatively uncracked alteration layer measuring approximately  $30 \mu\text{m}$  by both techniques (Figures 4, 7a). The alteration layers appear parallel to the surface, and, in some areas of the OCT data, defined by a faint rather than bright line, possibly suggesting a hydrated glass/bulk glass interface that has not yet delaminated. A third area measured on DCM 717 by OCT exhibits an alteration layer approximately  $66 \mu\text{m}$  thick (not shown), which is remarkably similar to that measured on the F-1 seven-day aged sample. This

demonstrates how alteration layers can vary from one region to the next, and underlines the value of non-invasive analysis in multiple areas.

OCT 2D profile images of DCM 1681 (Figure 7b), a severely deteriorated Laurent flute, indicate a thick, regular, and cracked alteration layer in some areas, as well as what could be called secondary alteration regimes that contain curving sub-surface cracks beneath the first alteration layer in other regions. OCT analysis shows that the primary alteration layers in all joints of this flute range from approximately  $60\text{--}80 \mu\text{m}$  in thickness, while secondary regimes exist up to  $175 \mu\text{m}$  below the surface. These deep cracks, sometimes parallel to the glass surface, pose potential issues for aqueous treatment of the glass. Imaging of spalled areas also shows that a new alteration layer has formed underneath the loss (Figure 7b). OCT images of the flute's interior surfaces obtained by focusing through a keyhole reveal a rougher glass surface, also with a cracked alteration layer approximately  $75 \mu\text{m}$  thick, parallel to and following the surface morphology (not shown).

## DISCUSSION

Taken together, evidence of alteration in the Laurent flutes and model glass samples clarifies the value of utilizing different methods for condition assessment of these 19<sup>th</sup>-century treasures. While advanced cracking is readily discernible, visual inspection and surface pH measurements can be confusing for assessment of earlier stages of deterioration in this type of potash glass, when intervention can be most effective. For example, the DCM 717 xFJ does not exhibit visible deterioration, but is found by BSE-SEM/EDS and OCT analysis to have an appreciable depletion layer, and by XRD to contain potassium reaction products in surface scrapings. This supports theoretical alkali silicate deterioration mechanisms in terms of replacement of alkali ions in the silicon dioxide matrix with water or hydroxides, although this type of glass may not manifest deterioration symptoms identical to sodium silicate glass (Vilarique et al. 2006; De Bardi et al. 2013; Rodrigues et al. 2018a; 2018b). On the other hand, analysis of surface particulates is useful for providing evidence of relatively benign residues on the glass surfaces that may be mistaken for deterioration products or a reactive surface.

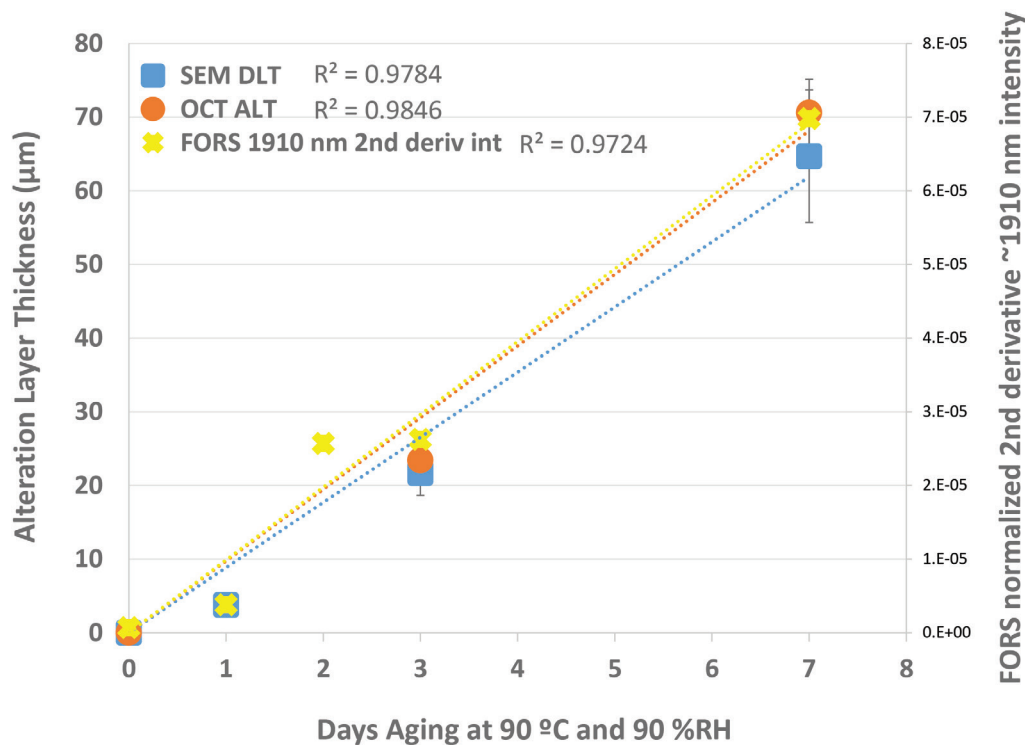


**Figure 8.** Overlaid plots of model potash glass F-1, crucible side, time of artificial aging vs. SEM depletion layer thickness (DLT) ( $\mu\text{m}$ ), OCT alteration layer thickness (ALT) ( $\mu\text{m}$ ), and FORS 2<sup>nd</sup>-derivative intensity derived from the peak near 1910 nm (normalized)

For reliable and non-invasive assessment of potash glass deterioration, OCT and FORS show excellent capabilities for determining alteration layer thickness, morphology, and cracking patterns. Together with BSE-SEM/EDS, results provide evidence that the hydration layer is coincident with the alkali-depleted layer on the microscale. Plots of alteration layer thickness for artificially aged model samples F-1, compared to normalized second-derivative FORS intensity derived from the peak near 1910 nm, show excellent correlation for kinetics of deterioration by all three techniques (Figure 8), where alteration thickness increases linearly with time of aging. Results from FORS are striking in their non-invasive detection of the earliest stages of deterioration in potash glass. OCT is particularly valuable for assessment of subsurface cracking before treatment is proposed.

## CONCLUSIONS

Results highlight the importance of using multiple tools to assess potash glass cultural heritage, represented here by Claude Laurent's 19<sup>th</sup>-century glass flutes. The condition of these beautiful musical instruments depends on their inherent instability, as well as their use and environmental history. Analytical results from BSE-SEM/EDS, FORS, and OCT provide highly complementary, specific information about the character of the alteration layer on individual flutes. Non-invasive FORS and OCT provide objective measurements of glass hydration and the morphology of the gel layer, in excellent agreement with BSE-SEM results from a microsample. Given the opportunity for sampling, accurate composition determination allows production and artificial aging of model glasses; these samples provide material for unrestricted examination, which can shed light on natural aging processes in the objects under investigation. Surface particulate analysis also aids visual assessment. Overall, analysis by the techniques discussed here can significantly advance our ability to assess the condition of historical glass and form preservation strategies.

## ACKNOWLEDGMENTS

The authors wish to acknowledge contributions from Nicholas Kivi, Ruhi Perez-Gokhale, Olivia Brum, Amelia Barberis, Andrea Kidder, Xiaogang Xie, Fernando Perez-Cardenas and Dana Hemmenway, as well as Mark Leone and multiple colleagues from museums holding Laurent flutes. The authors are grateful to the National Endowment for the Humanities Division of Preservation and Access for financial support.

## REFERENCES

- Brill, R.H. 1972. Incipient crizzling in some early glass. *Bulletin of the American Group. International Institute for Conservation of Historic and Artistic Works* 12(2): 46–47.
- Brill, R.H. 1975. Crizzling – A problem in glass conservation. In *Archaeology and the applied arts: Contributions to the 1975 IIC Congress, Stockholm*, 121–134. London: International Institute for Conservation of Historic and Artistic Works.
- Brostoff, L., C.L. Ward Bamford, T. Diba, A. Buechele, M. Loew, and J. Zara. In press. Optical coherence spectroscopy of 19<sup>th</sup> century glass: Facts and phantoms. *Proc. SPIE 11058-31*.
- Buechele, A., L. Brostoff, I. Muller, C.L. Ward-Bamford, and X. Xie. 2015. A study of glass composition and crizzling in two Claude Laurent glass flutes from the Library of Congress. *Microscopy and Microanalysis* 21(S3): 1161-1162. 1161–62.
- Bunker, B.C. 1994. Molecular mechanisms for corrosion of silica and silicate glasses. *Journal of Non-Crystalline Solids* 179: 300-308.
- Clark, D.E. and B.K. Zaitos. 1992. *Corrosion of glass, ceramics and ceramic superconductors: Principles, testing, characterization and applications*. Park Ridge: Noyes Publications.
- Clark, R.N. 1999. Spectroscopy of rocks and minerals, and principles of spectroscopy. In *Manual of remote sensing, volume 3: Remote sensing for the earth sciences*, ed. A.N. Rencz, 3-58. New York: John Wiley and Sons.
- De Bardi, M., R. Wiesinger, and M. Schreiner. 2013. Leaching studies of potash–lime–silica glass with medieval composition by IRRAS. *Journal of Non-Crystalline Solids* 360: 57–63.
- Farges, F., M.-P. Etcheverry, A. Haddi, P. Trocellier, E. Curti, and G.E. Brown. 2006. Durability of silicate glasses: An historical approach. In *Proceeding of the 13th International Conference on X-ray Absorption Fine Structure (XAFS13), 9-14 July 2006*, eds. B. Hedman and P. Pianetta. Stanford: Stanford Synchrotron Radiation Laboratory. [http://www.slac.stanford.edu/econf/C060709/papers/008\\_THPL1.PDF](http://www.slac.stanford.edu/econf/C060709/papers/008_THPL1.PDF) (accessed 27 September 2017).
- Fearn, S., D.S. McPhail, B.Hagenhoff, and E. Tallarek. 2006. TOF-SIMS analysis of corroding museum glass. *Applied Surface Science* 252(19): 7136-7139.
- Fletcher, P.J., I. Freestone, and R. Geschke. 2008. Analysis and conservation of a weeping glass scarab. *The British Museum Technical Research Bulletin* 2. [http://britishmuseum.org/research/publications/online\\_journals/technical\\_research\\_bulletin/bmtrb\\_volume\\_2.aspx](http://britishmuseum.org/research/publications/online_journals/technical_research_bulletin/bmtrb_volume_2.aspx) (accessed 6 June 2014).
- Hench, L.L. and D.E. Clark. 1978. Physical chemistry of glass surfaces. *Journal of Non-Crystalline Solids* 28: 83-105.
- Koob, S.P. 2004. Cleaning glass: A many-faceted issue. In *Objects specialty group postprints, volume II, 2004*, eds. V. Greene and P. Griffin, 60-70. Washington, DC: The American Institute for Conservation of Historic and Artistic Works.
- Koob, S.P. 2006. *Conservation and care of glass objects*. London: Archetype Publications in association with The Corning Museum of Glass
- Koob, S.P. 2012. Crizzling glasses: Problems and solutions. *European Journal of Glass Science and Technology Part A Glass Technology* 53(5): 189–191.
- Koob, S.P., J.J. Kunicki-Goldfinger, and R.H. Brill. 2018. Caring for glass collections: The importance of maintaining environmental controls. *Studies in Conservation* 63(sup1): 146-150.
- Kunicki-Goldfinger, J.J. 2002. Preventive conservation strategy for glass collections; Identification of glass objects susceptible to crizzling. In *Proceedings of the 5th EC conference cultural heritage research: A pan-European challenge: May 16-18, 2002, Cracow, Poland*, ed. R. Kozlowski, 301–304. Kraków: Institute of Catalysis and Surface Chemistry, Polish Academy of Sciences.

- Kunicki-Goldfinger, J.J. 2008. Unstable historic glass: Symptoms, causes, mechanisms and conservation. *Studies in Conservation* 53(sup2): 47–60.
- Kunicki-Goldfinger, J.J., P. Targowski, M. Gora, and P. Karaszkiwicz. 2009. Characterization of glass surface morphology by optical coherence tomography. *Studies in Conservation* 54(2): 117-128.
- Laurent Glass Flutes. Library of Congress. <https://www.loc.gov/collections/dayton-c-miller-collection/articles-and-essays/laurent-glass-flutes/> (accessed 5 July 2016).
- Laurent Patent 1806. Library of Congress. <https://www.loc.gov/collections/static/dayton-c-miller-collection/images/laurent-patent-1806-translation.pdf> (accessed 5 July 2016).
- Newton, R.G. and S. Davison. 2003. *Conservation of glass*. Second edition. Oxford: Butterworth-Heinemann.
- Palomar, T., A. Chabas, D.M. Bastidas, D. de la Fuente, and A. Verney-Carron. 2017. Effect of marine aerosols on the alteration of silicate glasses. *Journal of Non-Crystalline Solids* 471: 328-337.
- Rice, M.S., E.A. Cloutis, J.F. Bell, D.L. Bish, B.H. Horgan, S.A. Mertzman, M.A. Craig, R.W. Renaut, B. Gautason, and B. Mountain. 2013. Reflectance spectra diversity of silica-rich materials: Sensitivity to environment and implications for detections on Mars. *Icarus* 223(1): 499-533.
- Rodrigues, A., S. Fearn, T. Palomar, and M. Vilarigues. 2018a. Early stages of surface alteration of soda-rich-silicate glasses in the museum environment. *Corrosion Science* 143: 362-375.
- Rodrigues, A., S. Fearn, M. Vilarigues. 2018b. Historic K-rich silicate glass surface alteration: Behaviour of high-silica content matrices. *Corrosion Science* 145: 249-261.
- Ryan, J. 1995. Chemical stabilisation of weathered glass surfaces. *V&A Conservation Journal* 16. <http://www.vam.ac.uk/content/journals/conservation-journal/issue-16/chemical-stabilisation-of-weathered-glass-surfaces/> (accessed 6 June 2014).
- Vilariques, M. and R.C. da Silva. 2006. Characterization of potash-glass corrosion in aqueous solution by ion beam and IR spectroscopy. *Journal of Non-crystalline Solids* 352: 5368-5375.
- Ward-Bamford, C.L., L. Brostoff, I. Muller, and S. Zaleski. 2018. Collaborative technical study of Claude Laurent's glass flutes. Oral presentation in Science Meets Music symposium, 10 April 2018, "Library of Congress, Washington, DC, United States of America. <http://www.loc.gov/preservation/outreach/tops/music/index.html?loclr=eapn> (accessed 17 July 2019).
- Ward-Bamford, C.L., L. Brostoff, D. Klein, N. Kivi, R. Perez, I.S. Muller, A.C. Buechele, F. France, and M. Loew. 2019. A new, simplified approach for assessing glass musical instruments. *CIMCIM Bulletin*: 6-12.
- White, W.B. 1992. Theory of corrosion in glass and ceramics. In *Corrosion of glass, ceramics and ceramic superconductors: Principles, testing, characterization and applications*, eds. D.E. Clark and B.K. Zoitos. Park Ridge: Noyes Publications.
- Zaleski, S., E. Montagnino, L. Brostoff, I. Muller, A. Buechele, C.L. Ward Bamford, F. France, and M. Loew. 2019. Application of fiber optic reflectance spectroscopy for the detection of historical glass deterioration. *Journal of the American Ceramic Society*.